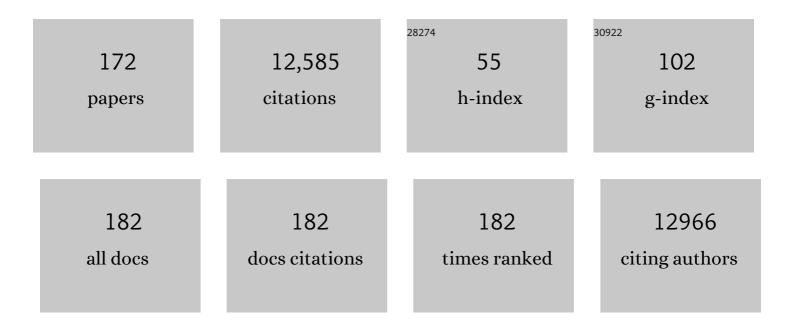
## David G Norris

List of Publications by Year in descending order

Source: https://exaly.com/author-pdf/4167138/publications.pdf Version: 2024-02-01



DAVID C. NOPPIS

#	Article	IF	CITATIONS
1	Systematic validation of structural brain networks in cerebral small vessel disease. Journal of Cerebral Blood Flow and Metabolism, 2022, 42, 1020-1032.	4.3	9
2	Multi-shell Diffusion MRI Models for White Matter Characterization in Cerebral Small Vessel Disease. Neurology, 2021, 96, e698-e708.	1.1	33
3	Estimation of laminar BOLD activation profiles using deconvolution with a physiological point spread function. Journal of Neuroscience Methods, 2021, 353, 109095.	2.5	10
4	This house proposes that low field and high field MRI are by destiny worst enemies, and can never be the best of friends!. Magnetic Resonance Materials in Physics, Biology, and Medicine, 2021, 34, 475-477.	2.0	1
5	An in-vivo study of BOLD laminar responses as a function of echo time and static magnetic field strength. Scientific Reports, 2021, 11, 1862.	3.3	6
6	Report on the hot topic debate at ESMRMB 2021. Magnetic Resonance Materials in Physics, Biology, and Medicine, 2021, 34, 775-778.	2.0	0
7	Structural network changes in cerebral small vessel disease. Journal of Neurology, Neurosurgery and Psychiatry, 2020, 91, 196-203.	1.9	28
8	Single-subject Single-session Temporally-Independent Functional Modes of Brain Activity. NeuroImage, 2020, 218, 116783.	4.2	3
9	Functional connectivity of the Precuneus reflects effectiveness of visual restitution training in chronic hemianopia. NeuroImage: Clinical, 2020, 27, 102292.	2.7	11
10	A half-century of innovation in technology—preparing MRI for the 21st century. British Journal of Radiology, 2020, 93, 20200113.	2.2	15
11	Structural network efficiency predicts cognitive decline in cerebral small vessel disease. NeuroImage: Clinical, 2020, 27, 102325.	2.7	17
12	Alterations and test–retest reliability of functional connectivity network measures in cerebral small vessel disease. Human Brain Mapping, 2020, 41, 2629-2641.	3.6	19
13	The contribution of acute infarcts to cerebral small vessel disease progression. Annals of Neurology, 2019, 86, 582-592.	5.3	27
14	Laminar signal extraction over extended cortical areas by means of a spatial GLM. PLoS ONE, 2019, 14, e0212493.	2.5	24
15	Higher GABA concentration in the medial prefrontal cortex of Type 2 diabetes patients is associated with episodic memory dysfunction. Human Brain Mapping, 2019, 40, 4287-4295.	3.6	22
16	A comparison of sLASER and MEGA-sLASER using simultaneous interleaved acquisition for measuring GABA in the human brain at 7T. PLoS ONE, 2019, 14, e0223702.	2.5	21
17	Fast modelâ€based T <sub>2</sub> mapping using SARâ€reduced simultaneous multislice excitation. Magnetic Resonance in Medicine, 2019, 82, 2090-2103.	3.0	11
18	Laminar specific fMRI reveals directed interactions in distributed networks during language processing. Proceedings of the National Academy of Sciences of the United States of America, 2019, 116, 21185-21190.	7.1	62

#	Article	IF	CITATIONS
19	The role of small diffusion-weighted imaging lesions in cerebral small vessel disease. Neurology, 2019, 93, 10.1212/WNL.000000000008364.	1.1	14
20	Effect of linewidth on estimation of metabolic concentration when using water lineshape spectral model fitting for single voxel proton spectroscopy at 7â€T. Journal of Magnetic Resonance, 2019, 304, 53-61.	2.1	5
21	Laminar (f)MRI: A short history and future prospects. NeuroImage, 2019, 197, 643-649.	4.2	45
22	Improved cortical boundary registration for locally distorted fMRI scans. PLoS ONE, 2019, 14, e0223440.	2.5	6
23	Brain atrophy and strategic lesion location increases risk of parkinsonism in cerebral small vessel disease. Parkinsonism and Related Disorders, 2019, 61, 94-100.	2.2	2
24	Memory decline in elderly with cerebral small vessel disease explained by temporal interactions between white matter hyperintensities and hippocampal atrophy. Hippocampus, 2019, 29, 500-510.	1.9	28
25	Similar Subgroups Based on Cognitive Performance Parse Heterogeneity in Adults With ADHD and Healthy Controls. Journal of Attention Disorders, 2018, 22, 281-292.	2.6	40
26	The increase in medial prefrontal glutamate/glutamine concentration during memory encoding is associated with better memory performance and stronger functional connectivity in the human medial prefrontal–thalamus–hippocampus network. Human Brain Mapping, 2018, 39, 2381-2390.	3.6	23
27	Clinical application of Half Fourier Acquisition Single Shot Turbo Spin Echo (HASTE) imaging accelerated by simultaneous multi-slice acquisition. European Journal of Radiology, 2018, 98, 200-206.	2.6	7
28	Progression of White Matter Hyperintensities Preceded by Heterogeneous Decline of Microstructural Integrity. Stroke, 2018, 49, 1386-1393.	2.0	66
29	Introductory editorial. Magnetic Resonance Materials in Physics, Biology, and Medicine, 2018, 31, 1-2.	2.0	2
30	How to choose the right MR sequence for your research question at 7 T and above?. NeuroImage, 2018, 168, 119-140.	4.2	41
31	Implications of the magnetic susceptibility difference between grey and white matter for single-voxel proton spectroscopy at 7â€T. Journal of Magnetic Resonance, 2018, 297, 51-60.	2.1	2
32	Risk of Nursing Home Admission in Cerebral Small Vessel Disease. Stroke, 2018, 49, 2659-2665.	2.0	3
33	Laminar Organization of Working Memory Signals in Human Visual Cortex. Current Biology, 2018, 28, 3435-3440.e4.	3.9	71
34	Structure tensor informed fibre tractography at 3T. Human Brain Mapping, 2018, 39, 4440-4451.	3.6	4
35	Pros and cons of ultra-high-field MRI/MRS for human application. Progress in Nuclear Magnetic Resonance Spectroscopy, 2018, 109, 1-50.	7.5	331
36	Investigating the origin and evolution of cerebral small vessel disease: The RUN DMC – InTENse study. European Stroke Journal, 2018, 3, 369-378.	5.5	14

#	Article	IF	CITATIONS
37	MASEâ€sLASER, a shortâ€TE, matched chemical shift displacement error sequence for singleâ€voxel spectroscopy at ultrahigh field. NMR in Biomedicine, 2018, 31, e3940.	2.8	1
38	Porcupine: A visual pipeline tool for neuroimaging analysis. PLoS Computational Biology, 2018, 14, e1006064.	3.2	12
39	Multiband echoâ€ <b>s</b> hifted echo planar imaging. Magnetic Resonance in Medicine, 2017, 77, 1981-1986.	3.0	9
40	Abnormal connectivity in the sensorimotor network predicts attention deficits in traumatic brain injury. Experimental Brain Research, 2017, 235, 799-807.	1.5	45
41	Disruption of rich club organisation in cerebral small vessel disease. Human Brain Mapping, 2017, 38, 1751-1766.	3.6	64
42	Nonlinear temporal dynamics of cerebral small vessel disease. Neurology, 2017, 89, 1569-1577.	1.1	89
43	Baseline Cerebral Small Vessel Disease Is Not Associated with Gait Decline After Five Years. Movement Disorders Clinical Practice, 2017, 4, 374-382.	1.5	8
44	Aerobic Activity in the Healthy Elderly Is Associated with Larger Plasticity in Memory Related Brain Structures and Lower Systemic Inflammation. Frontiers in Aging Neuroscience, 2016, 08, 319.	3.4	16
45	Recommended responsibilities for management of MR safety. Journal of Magnetic Resonance Imaging, 2016, 44, 1067-1069.	3.4	28
46	Multiband multislab 3 <scp>D</scp> timeâ€ofâ€flight magnetic resonance angiography for reduced acquisition time and improved sensitivity. Magnetic Resonance in Medicine, 2016, 75, 1662-1668.	3.0	21
47	The traveling heads: multicenter brain imaging at 7 Tesla. Magnetic Resonance Materials in Physics, Biology, and Medicine, 2016, 29, 399-415.	2.0	26
48	Structural network connectivity and cognition in cerebral small vessel disease. Human Brain Mapping, 2016, 37, 300-310.	3.6	122
49	Simultaneous multislice (SMS) imaging techniques. Magnetic Resonance in Medicine, 2016, 75, 63-81.	3.0	420
50	The relationship between oscillatory EEG activity and the laminar-specific BOLD signal. Proceedings of the United States of America, 2016, 113, 6761-6766.	7.1	147
51	Selective Activation of the Deep Layers of the Human Primary Visual Cortex by Top-Down Feedback. Current Biology, 2016, 26, 371-376.	3.9	310
52	Structural network efficiency predicts conversion to dementia. Neurology, 2016, 86, 1112-1119.	1.1	103
53	Characterising resting-state functional connectivity in a large sample of adults with ADHD. Progress in Neuro-Psychopharmacology and Biological Psychiatry, 2016, 67, 82-91.	4.8	53
54	Factors Associated With 8-Year Mortality in Older Patients With Cerebral Small Vessel Disease. JAMA Neurology, 2016, 73, 402.	9.0	43

#	Article	IF	CITATIONS
55	A cortical vascular model for examining the specificity of the laminar BOLD signal. NeuroImage, 2016, 132, 491-498.	4.2	136
56	White Matter and Hippocampal Volume Predict the Risk of Dementia in Patients withÂCerebral Small Vessel Disease: TheÂRUN DMC Study. Journal of Alzheimer's Disease, 2015, 49, 863-873.	2.6	40
57	Relationship Between White Matter Hyperintensities, Cortical Thickness, and Cognition. Stroke, 2015, 46, 425-432.	2.0	147
58	Diffusion tensor characteristics of gyrencephaly using high resolution diffusion MRI in vivo at 7T. NeuroImage, 2015, 109, 378-387.	4.2	59
59	Improved sensitivity and specificity for resting state and task fMRI with multiband multi-echo EPI compared to multi-echo EPI at 7 T. NeuroImage, 2015, 119, 352-361.	4.2	58
60	White Matter Integrity and Depressive Symptoms in Cerebral Small Vessel Disease: The RUN DMC Study. American Journal of Geriatric Psychiatry, 2015, 23, 525-535.	1.2	46
61	Cohort study ON Neuroimaging, Etiology and Cognitive consequences of Transient neurological attacks (CONNECT): study rationale and protocol. BMC Neurology, 2015, 15, 36.	1.8	7
62	Cerebral small vessel disease and incident parkinsonism. Neurology, 2015, 85, 1569-1577.	1.1	85
63	White matter integrity in small vessel disease is related to cognition. NeuroImage: Clinical, 2015, 7, 518-524.	2.7	143
64	L2-Proficiency-Dependent Laterality Shift in Structural Connectivity of Brain Language Pathways. Brain Connectivity, 2015, 5, 349-361.	1.7	24
65	Pulse Sequences for fMRI. Biological Magnetic Resonance, 2015, , 131-162.	0.4	3
66	BOLD fMRI signal characteristics of S1- and S2-SSFP at 7 Tesla. Frontiers in Neuroscience, 2014, 8, 49.	2.8	21
67	Occipital Alpha Activity during Stimulus Processing Gates the Information Flow to Object-Selective Cortex. PLoS Biology, 2014, 12, e1001965.	5.6	175
68	Application of PINS radiofrequency pulses to reduce power deposition in RARE/turbo spin echo imaging of the human head. Magnetic Resonance in Medicine, 2014, 71, 44-49.	3.0	42
69	Whole brain, high resolution multiband spin-echo EPI fMRI at 7T: A comparison with gradient-echo EPI using a color-word Stroop task. NeuroImage, 2014, 97, 142-150.	4.2	42
70	Slice accelerated diffusionâ€weighted imaging at ultraâ€high field strength. Magnetic Resonance in Medicine, 2014, 71, 1518-1525.	3.0	41
71	Simultaneous multislice inversion contrast imaging using power independent of the number of slices (PINS) and delays alternating with nutation for tailored excitation (DANTE) radio frequency pulses. Magnetic Resonance in Medicine, 2013, 69, 1670-1676.	3.0	14
72	Physical activity is related to the structural integrity of cerebral white matter. Neurology, 2013, 81, 971-976.	1.1	76

5

#	Article	IF	CITATIONS
73	Superselective arterial spin labeling applied for flow territory mapping in various cerebrovascular diseases. Journal of Magnetic Resonance Imaging, 2013, 38, 496-503.	3.4	31
74	Memoryâ€Related Hippocampal Activity Can Be Measured Robustly Using fMRI at 7 Tesla. Journal of Neuroimaging, 2013, 23, 445-451.	2.0	23
75	Default Mode Network Connectivity in Stroke Patients. PLoS ONE, 2013, 8, e66556.	2.5	87
76	Topographic Hub Maps of the Human Structural Neocortical Network. PLoS ONE, 2013, 8, e65511.	2.5	46
77	Hypertension is Related to the Microstructure of the Corpus Callosum: The RUN DMC Study. Journal of Alzheimer's Disease, 2012, 32, 623-631.	2.6	38
78	The Structural Connectivity Underpinning Language Aptitude, Working Memory, and IQ in the Perisylvian Language Network. Language Learning, 2012, 62, 110-130.	2.7	43
79	Structure Tensor Informed Fiber Tractography (STIFT) by combining gradient echo MRI and diffusion weighted imaging. NeuroImage, 2012, 59, 3941-3954.	4.2	17
80	Diffusion tensor imaging and mild parkinsonian signs in cerebral small vessel disease. Neurobiology of Aging, 2012, 33, 2106-2112.	3.1	15
81	Diffusion tensor imaging and cognition in cerebral small vessel disease. Biochimica Et Biophysica Acta - Molecular Basis of Disease, 2012, 1822, 401-407.	3.8	79
82	Spin-echo fMRI: The poor relation?. NeuroImage, 2012, 62, 1109-1115.	4.2	72
83	Whole brain, high resolution spin-echo resting state fMRI using PINS multiplexing at 7T. NeuroImage, 2012, 62, 1939-1946.	4.2	56
84	Selective multivessel labeling approach for perfusion territory imaging in pseudoâ€continuous arterial spin labeling. Magnetic Resonance in Medicine, 2012, 68, 214-219.	3.0	12
85	Abnormal whole-brain functional networks in homogeneous acute mild traumatic brain injury. Neurology, 2012, 79, 175-182.	1.1	148
86	Diffusion tensor imaging of the hippocampus and verbal memory performance: The RUN DMC Study. Human Brain Mapping, 2012, 33, 542-551.	3.6	39
87	Multi-echo fMRI of the cortical laminae in humans at 7T. NeuroImage, 2011, 56, 1276-1285.	4.2	152
88	Neuronal Dynamics Underlying High- and Low-Frequency EEG Oscillations Contribute Independently to the Human BOLD Signal. Neuron, 2011, 69, 572-583.	8.1	408
89	Risk factors and prognosis of young stroke. The FUTURE study: A prospective cohort study. Study rationale and protocol. BMC Neurology, 2011, 11, 109.	1.8	51
90	Causes and consequences of cerebral small vessel disease. The RUN DMC study: a prospective cohort study. Study rationale and protocol. BMC Neurology, 2011, 11, 29.	1.8	154

#	Article	IF	CITATIONS
91	Power independent of number of slices (PINS) radiofrequency pulses for lowâ€power simultaneous multislice excitation. Magnetic Resonance in Medicine, 2011, 66, 1234-1240.	3.0	110
92	Perfusion territory imaging of intracranial branching arteries – optimization of continuous arteryâ€selective spin labeling (CASSL). NMR in Biomedicine, 2011, 24, 404-412.	2.8	9
93	Exploring the postâ€stimulus undershoot with spinâ€echo fMRI: Implications for models of neurovascular response. Human Brain Mapping, 2011, 32, 141-153.	3.6	15
94	Application of wholeâ€brain CBVâ€weighted fMRI to a cognitive stimulation paradigm: Robust activation detection in a stroop task experiment using 3D GRASE VASO. Human Brain Mapping, 2011, 32, 974-981.	3.6	22
95	Diffusion Tensor Imaging and Gait in Elderly Persons With Cerebral Small Vessel Disease. Stroke, 2011, 42, 373-379.	2.0	53
96	Cigarette smoking is associated with reduced microstructural integrity of cerebral white matter. Brain, 2011, 134, 2116-2124.	7.6	139
97	Loss of white matter integrity is associated with gait disorders in cerebral small vessel disease. Brain, 2011, 134, 73-83.	7.6	246
98	Modulation of Visually Evoked Cortical fMRI Responses by Phase of Ongoing Occipital Alpha Oscillations. Journal of Neuroscience, 2011, 31, 3813-3820.	3.6	126
99	Hypertension and Cerebral Diffusion Tensor Imaging in Small Vessel Disease. Stroke, 2010, 41, 2801-2806.	2.0	76
100	Functional connectivity between brain regions involved in learning words of a new language. Brain and Language, 2010, 113, 21-27.	1.6	87
101	Layerâ€specific BOLD activation in human V1. Human Brain Mapping, 2010, 31, 1297-1304.	3.6	190
102	<i>T</i> <sub>2</sub> -weighted 3D fMRI using <i>S</i> <sub>2</sub> -SSFP at 7 tesla. Magnetic Resonance in Medicine, 2010, 63, 1015-1020.	3.0	34
103	Superselective pseudocontinuous arterial spin labeling. Magnetic Resonance in Medicine, 2010, 64, 777-786.	3.0	65
104	Topographical Functional Connectivity Pattern in the Perisylvian Language Networks. Cerebral Cortex, 2010, 20, 549-560.	2.9	176
105	Persistent schema-dependent hippocampal-neocortical connectivity during memory encoding and postencoding rest in humans. Proceedings of the National Academy of Sciences of the United States of America, 2010, 107, 7550-7555.	7.1	383
106	3D singleâ€ <b>s</b> hot VASO using a maxwell gradient compensated GRASE sequence. Magnetic Resonance in Medicine, 2009, 62, 255-262.	3.0	34
107	A dual echo approach to removing motion artefacts in fMRI time series. NMR in Biomedicine, 2009, 22, 551-560.	2.8	33
108	Investigating the benefits of multi-echo EPI for fMRI at 7ÂT. NeuroImage, 2009, 45, 1162-1172.	4.2	121

#	Article	IF	CITATIONS
109	Trial-by-trial coupling between EEG and BOLD identifies networks related to alpha and theta EEG power increases during working memory maintenance. NeuroImage, 2009, 44, 1224-1238.	4.2	313
110	Extraction of Task-Related Activation From Multi-Echo BOLD fMRI. IEEE Journal on Selected Topics in Signal Processing, 2008, 2, 954-964.	10.8	10
111	Frontal theta EEG activity correlates negatively with the default mode network in resting state. International Journal of Psychophysiology, 2008, 67, 242-251.	1.0	348
112	Probabilistic Inference on Q-ball Imaging Data. IEEE Transactions on Medical Imaging, 2007, 26, 1515-1524.	8.9	12
113	Inability to directly detect magnetic field changes associated with neuronal activity. Magnetic Resonance in Medicine, 2007, 57, 411-416.	3.0	62
114	Selective parity RARE imaging. Magnetic Resonance in Medicine, 2007, 58, 643-649.	3.0	19
115	Fast spin echo sequences for BOLD functional MRI. Magnetic Resonance Materials in Physics, Biology, and Medicine, 2007, 20, 11-17.	2.0	59
116	Measurement of activation-related changes in cerebral blood volume: VASO with single-shot HASTE acquisition. Magnetic Resonance Materials in Physics, Biology, and Medicine, 2007, 20, 63-67.	2.0	22
117	Combining EEG and fMRI to investigate the post-movement beta rebound. NeuroImage, 2006, 29, 685-696.	4.2	130
118	Playing it too safe?. Nature Physics, 2006, 2, 358-360.	16.7	2
119	BOLD contrast sensitivity enhancement and artifact reduction with multiecho EPI: Parallel-acquired inhomogeneity-desensitized fMRI. Magnetic Resonance in Medicine, 2006, 55, 1227-1235.	3.0	399
120	Principles of magnetic resonance assessment of brain function. Journal of Magnetic Resonance Imaging, 2006, 23, 794-807.	3.4	153
121	Continuous arterial spin labeling at the human common carotid artery: the influence of transit times. NMR in Biomedicine, 2005, 18, 19-23.	2.8	25
122	A comparison of signal instability in 2D and 3D EPI resting-state fMRI. NMR in Biomedicine, 2005, 18, 534-542.	2.8	20
123	Is there a change in water proton density associated with functional magnetic resonance imaging?. Magnetic Resonance in Medicine, 2005, 53, 470-473.	3.0	25
124	Improving the amplitude-modulated control experiment for multislice continuous arterial spin labeling. Magnetic Resonance in Medicine, 2005, 53, 1096-1102.	3.0	21
125	Continuous arteryâ€selective spin labeling (CASSL). Magnetic Resonance in Medicine, 2005, 53, 1006-1012.	3.0	52
126	Quantifying the spatial resolution of the gradient echo and spin echo BOLD response at 3 Tesla. Magnetic Resonance in Medicine, 2005, 54, 1465-1472.	3.0	163

#	Article	IF	CITATIONS
127	Efficiency of flow-driven adiabatic spin inversion under realistic experimental conditions: A computer simulation. Magnetic Resonance in Medicine, 2004, 51, 1187-1193.	3.0	29
128	Quantifying the intra- and extravascular contributions to spin-echo fMRI at 3 T. Magnetic Resonance in Medicine, 2004, 52, 724-732.	3.0	68
129	Advances in High-Field Magnetic Resonance Imaging. Annual Review of Biomedical Engineering, 2004, 6, 157-184.	12.3	101
130	Reduced BOLD response to periodic visual stimulation. NeuroImage, 2004, 21, 236-243.	4.2	43
131	High field human imaging. Journal of Magnetic Resonance Imaging, 2003, 18, 519-529.	3.4	166
132	Functional perfusion imaging using continuous arterial spin labeling with separate labeling and imaging coils at 3 T. Magnetic Resonance in Medicine, 2003, 49, 791-795.	3.0	56
133	Determination of Cerebrovascular Reactivity by Means of fMRI Signal Changes in Cerebral Microangiopathy: A Correlation with Morphological Abnormalities. Cerebrovascular Diseases, 2003, 16, 158-165.	1.7	30
134	An Investigation of the Value of Spin-Echo-Based fMRI Using a Stroop Color–Word Matching Task and EPI at 3 T. NeuroImage, 2002, 15, 719-726.	4.2	118
135	An Investigation of Functional and Anatomical Connectivity Using Magnetic Resonance Imaging. NeuroImage, 2002, 16, 241-250.	4.2	443
136	Characterization of cerebral microangiopathy using 3 Tesla MRI: Correlation with neurological impairment and vascular risk factors. Journal of Magnetic Resonance Imaging, 2002, 15, 1-7.	3.4	14
137	Continuous arterial spin labeling using a local magnetic field gradient coil. Magnetic Resonance in Medicine, 2002, 48, 543-546.	3.0	42
138	Adiabatic radiofrequency pulse forms in biomedical nuclear magnetic resonance. Concepts in Magnetic Resonance, 2002, 14, 89-101.	1.3	50
139	Single-shot curved slice imaging. Magnetic Resonance Materials in Physics, Biology, and Medicine, 2002, 14, 50-55.	2.0	6
140	Characterization of Cerebral Small Vessel Disease by Proton Spectroscopy and Morphological Magnetic Resonance. Cerebrovascular Diseases, 2001, 12, 82-90.	1.7	21
141	Implications of bulk motion for diffusion-weighted imaging experiments: Effects, mechanisms, and solutions. Journal of Magnetic Resonance Imaging, 2001, 13, 486-495.	3.4	92
142	Online motion correction for diffusion-weighted imaging using navigator echoes: Application to RARE imaging without sensitivity loss. Magnetic Resonance in Medicine, 2001, 45, 729-733.	3.0	44
143	A qualitative test of the balloon model for BOLD-based MR signal changes at 3T. Magnetic Resonance in Medicine, 2001, 46, 891-899.	3.0	53
144	The effects of microscopic tissue parameters on the diffusion weighted magnetic resonance imaging experiment. NMR in Biomedicine, 2001, 14, 77-93.	2.8	202

#	Article	IF	CITATIONS
145	Reduced power multislice MDEFT imaging. Journal of Magnetic Resonance Imaging, 2000, 11, 445-451.	3.4	151
146	An assessment of eddy current sensitivity and correction in single-shot diffusion-weighted imaging. Physics in Medicine and Biology, 2000, 45, 3821-3832.	3.0	42
147	Velocity Selective Radiofrequency Pulse Trains. Journal of Magnetic Resonance, 1999, 137, 231-236.	2.1	56
148	Application of double voxel functional spectroscopy to event-related cognitive experiments. Magnetic Resonance in Medicine, 1999, 41, 217-223.	3.0	10
149	A novel fast split-echo multi-shot diffusion-weighted MRI method using navigator echoes. Magnetic Resonance in Medicine, 1999, 41, 734-742.	3.0	26
150	Characterization of Middle Cerebral Artery Occlusion Infarct Development in the Rat Using Fast Nuclear Magnetic Resonance Proton Spectroscopic Imaging and Diffusion-Weighted Imaging. Journal of Cerebral Blood Flow and Metabolism, 1998, 18, 749-757.	4.3	24
151	GRASE imaging at 3 Tesla with template interactive phase–encoding. Magnetic Resonance in Medicine, 1998, 39, 970-979.	3.0	12
152	Use of Short Intertrial Intervals in Single-Trial Experiments: A 3T fMRI-Study. NeuroImage, 1998, 8, 327-339.	4.2	32
153	Mechanism and echo time dependence of the fast response in FMR. Magnetic Resonance in Medicine, 1997, 38, 1-6.	3.0	6
154	Fast proton spectroscopic imaging employing <i>k</i> â€space weighting achieved by variable repetition times. Magnetic Resonance in Medicine, 1996, 35, 457-464.	3.0	32
155	Biexponential diffusion attenuation in various states of brain tissue: Implications for diffusion-weighted imaging. Magnetic Resonance in Medicine, 1996, 36, 847-857.	3.0	534
156	Interpretation of DW-NMR data: Dependence on experimental conditions. NMR in Biomedicine, 1995, 8, 280-288.	2.8	29
157	Evolution of Regional Changes in Apparent Diffusion Coefficient during Focal Ischemia of Rat Brain: The Relationship of Quantitative Diffusion NMR Imaging to Reduction in Cerebral Blood Flow and Metabolic Disturbances. Journal of Cerebral Blood Flow and Metabolism, 1995, 15, 1002-1011.	4.3	304
158	Magnetization transfer affects the proton creatine/phosphocreatine signal intensity:In vivo demonstration in the rat brain. Magnetic Resonance in Medicine, 1994, 31, 81-84.	3.0	57
159	Detection of apparent restricted diffusion in healthy rat brain at short diffusion times. Magnetic Resonance in Medicine, 1994, 32, 672-677.	3.0	65
160	Healthy and infarcted brain tissues studied at short diffusion times: The origins of apparent restriction and the reduction in apparent diffusion coefficient. NMR in Biomedicine, 1994, 7, 304-310.	2.8	139
161	Early changes in apparent diffusion coefficient of rat brain following total circulatory arrest. Magnetic Resonance Materials in Physics, Biology, and Medicine, 1994, 2, 39-42.	2.0	9
162	Fast proton spectroscopic imaging using the slicedk-space method. Magnetic Resonance in Medicine, 1993, 30, 641-645.	3.0	46

#	Article	IF	CITATIONS
163	Dynamic imaging with contrast using U-FLARE. Magnetic Resonance Imaging, 1993, 11, 921-924.	1.8	14
164	On the application of ultra-fast rare experiments. Magnetic Resonance in Medicine, 1992, 27, 142-164.	3.0	172
165	T1 snapshot flash measurement of rat brain glioma: kinetics of the tumor-enhancing contrast agent manganese (iii) tetraphenylporphine sulfonate. Magnetic Resonance in Medicine, 1992, 27, 201-213.	3.0	35
166	An analysis of the effects of short T2 values on the hyperbolic-secant pulse. Journal of Magnetic Resonance, 1991, 92, 94-101.	0.5	27
167	Excitation angle optimization for snapshot FLASH and a signal comparison with EPI. Journal of Magnetic Resonance, 1991, 91, 190-193.	0.5	4
168	Ultrafast Low-Angle RARE: U-FLARE. Magnetic Resonance in Medicine, 1991, 17, 539-542.	3.0	76
169	A simple method of generating variable T1 contrast images using temporally reordered phase encoding. Magnetic Resonance in Medicine, 1990, 15, 483-490.	3.0	37
170	Concomitant magnetic field gradients and their effects on imaging at low magnetic field strengths. Magnetic Resonance Imaging, 1990, 8, 33-37.	1.8	107
171	Variable excitation angle AFP pulses. Magnetic Resonance in Medicine, 1989, 9, 435-440.	3.0	11
172	Projective Fourier angiography. Magnetic Resonance in Medicine, 1988, 7, 1-10.	3.0	10